All-fiber Er-doped dissipative soliton laser based on evanescent field interaction with carbon nanotube saturable absorber

Ju Hee Im, Sun Young Choi, Fabian Rotermund, and Dong-Il Yeom*

Division of Energy Systems Research, Ajou University, 443-749 Suwon, South Korea
*diyeom@ajou.ac.kr

Abstract: We report on an Er-doped fiber pulse laser at large net normal dispersion cavity by employing a dispersion compensating fiber in combination with a single-walled carbon nanotube (SWCNT) saturable absorber. A SWCNT/polymer composite film uniformly spin-coated on the side-polished fiber is prepared for robust and efficient nonlinear interaction with evanescent fields in the waveguide expecting increase of optical and thermal damage threshold compared to previously reported direct coating of SWCNTs on fiber ferrules. The fabricated dissipative soliton fiber laser exhibits high average output power of 55.6 mW, corresponding to pulse energy about 2.35 nJ. Highly chirped 5.8 ps pulses are generated with a spectral bandwidth of 13.9 nm and compressed down to 226 fs using additional length of conventional optical fiber at extra-cavity.

References and links

1. U. Keller, "Recent developments in compact ultrafast lasers," Nature **424**(6950), 831–838 (2003).
2. M. E. Fermann, and I. Hartl, "Ultrafast Fiber Laser Technology," IEEE J. Sel. Top. Quantum Electron. **15**(1), 191–206 (2009).
3. G. P. Agrawal, *Applications of nonlinear fiber optics*, (Elsevier, 2008), Chap. 5.
4. U. Keller, K. J. Weingarten, F. X. Kärtner, D. Kopf, B. Braun, I. D. Jung, R. Fluck, C. Hönninger, N. Matuschek, and J. Aus der Au, "Semiconductor saturable absorber mirrors (SESAMs) for femtosecond to nanosecond pulse generation in solid-state lasers," IEEE J. Sel. Top. Quantum Electron. **2**(3), 435–453 (1996).
5. S. Y. Set, H. Yaguchi, Y. Tanaka, and M. Jablonski, "Ultrafast fiber pulsed lasers incorporating carbon nanotubes," IEEE J. Sel. Top. Quantum Electron. **10**(1), 137–146 (2004).
6. K. H. Fong, K. Kikuchi, C. S. Goh, S. Y. Set, R. Grange, M. Haiml, A. Schlatter, and U. Keller, "Solid-state Er:Yb:glass laser mode-locked by using single-wall carbon nanotube thin film," Opt. Lett. **32**(1), 38–40 (2007).
7. W. B. Cho, J. H. Yim, S. Y. Choi, S. Lee, U. Griebner, V. Petrov, and F. Rotermund, "Mode-locked self-starting Cr:forsterite laser using a single-walled carbon nanotube saturable absorber," Opt. Lett. **33**(21), 2449–2451 (2008).
8. S. Kivistö, T. Hakulinen, A. Kaskela, B. Aitchison, D. P. Brown, A. G. Nasibulin, E. I. Kauppinen, A. Härkönen, and O. G. Okhotnikov, "Carbon nanotube films for ultrafast broadband technology," Opt. Express **17**(4), 2358–2363 (2009).
9. K. Kieu, and M. Mansuripur, "Femtosecond laser pulse generation with a fiber taper embedded in carbon nanotube/polymer composite," Opt. Lett. **32**(15), 2242–2244 (2007).
10. Y.-W. Song, S. Yamashita, C. S. Goh, and S. Y. Set, "Carbon nanotube mode lockers with enhanced nonlinearity via evanescent field interaction in D-shaped fibers," Opt. Lett. **32**(2), 148–150 (2007).
11. A. Martinez, K. Zhou, I. Bennion, and S. Yamashita, "In-fiber microchannel device filled with a carbon nanotube dispersion for passive mode-lock lasing," Opt. Express **16**(20), 15425–15430 (2008).
12. S. Y. Choi, F. Rotermund, H. Jung, K. Oh, and D.-I. Yeom, "Femtosecond mode-locked fiber laser employing a hollow optical fiber filled with carbon nanotube dispersion as saturable absorber," Opt. Express **17**(24), 21788–21793 (2009).
13. Y.-W. Song, S. Yamashita, and S. Maruyama, "Single-walled carbon nanotubes for high-energy optical pulse formation," Appl. Phys. Lett. **92**(2), 021115 (2008).
14. G. P. Agrawal, *Nonlinear fiber optics*, (Elsevier, 2007), Chap. 5.
15. W. J. Tomlinson, R. H. Stolen, and A. M. Johnson, "Optical wave breaking of pulses in nonlinear optical fibers," Opt. Lett. **10**(9), 457–459 (1985).
16. F. Ö. Ilday, J. R. Buckley, W. G. Clark, and F. W. Wise, "Self-similar evolution of parabolic pulses in a laser," Phys. Rev. Lett. **92**(21), 213902 (2004).

17. A. Chong, J. Buckley, W. Renninger, and F. Wise, "All-normal-dispersion femtosecond fiber laser," Opt. Express **14**(21), 10095–10100 (2006).
18. K. Kieu, W. H. Renninger, A. Chong, and F. W. Wise, "Sub-100 fs pulses at watt-level powers from a dissipative-soliton fiber laser," Opt. Lett. **34**(5), 593–595 (2009).
19. A. Cabasse, B. Ortaç, G. Martel, A. Hideur, and J. Limpert, "Dissipative solitons in a passively mode-locked Er-doped fiber with strong normal dispersion," Opt. Express **16**(23), 19322–19329 (2008).
20. K. Kieu, and F. W. Wise, "Self-similar and stretched-pulse operation of erbium-doped fiber lasers with carbon nanotubes saturable absorber," presented at the Conference on Lasers and Electro-Optics (CLEO), Baltimore-Maryland, USA, 31 May. 2009.
21. Z. Sun, A. G. Rozhin, F. Wang, T. Hasan, D. Popa, W. O'Neill, and A. C. Ferrari, "A compact, high power, ultrafast laser mode-locked by carbon nanotubes," Appl. Phys. Lett. **95**(25), 253102 (2009).
22. N. Akhmediev, and A. Ankiewicz, *Dissipative Solitons* (Springer, Berlin Heidelberg, 2005).
23. N. Akhmediev, and A. Ankiewicz, *Dissipative Solitons: From Optics to Biology and Medicine* (Springer, Berlin Heidelberg, 2008).
24. J. M. Soto-Crespo, N. Akhmediev, and A. Ankiewicz, "Pulsating, creeping, and erupting solitons in dissipative systems," Phys. Rev. Lett. **85**(14), 2937–2940 (2000).
25. W. H. Renninger, A. Chong, and F. W. Wise, "Dissipative solitons in normal-dispersion fiber lasers," Phys. Rev. A **77**(2), 023814 (2008).
26. N. Akhmediev, J. M. Soto-Crespo, and Ph. Grelu, "Roadmap to ultra-short record high-energy pulses out of laser oscillators," Phys. Lett. A **372**(17), 3124–3128 (2008).
27. W. Chang, A. Ankiewicz, J. M. Soto-Crespo, and N. Akhmediev, "Dissipative soliton resonances in laser models with parameter management," J. Opt. Soc. Am. B **25**(12), 1972–1977 (2008).

1. Introduction

Passively mode-locked lasers generating ultrashort optical pulses are interesting for fundamental research as well as practical application in diverse fields including nonlinear optics, bio-medical research, optical frequency metrology and material processing [1]. Ultrafast fiber lasers, as a counterpart of bulk solid-state lasers, have been continuously investigated with great attention due to their advantages such as alignment-free structure, low cost, efficient heat dissipation and high spatial beam quality [2]. In mode-locked fiber lasers, an optical component whose response is fast enough and nonlinear to the incident optical pulse intensity is commonly used for passive mode-locking based on saturable absorption, additive pulse mode locking or nonlinear polarization evolution (NPE) [3]. In practice, saturable absorption elements are popularly used for environmentally robust and stable laser mode-locking. For example, semiconductor saturable absorber mirrors (SESAMs) [4] are currently widespread mode-locking device in a variety of commercial fiber laser systems.

Recent development of novel saturable absorbers (SAs) based on single-walled carbon nanotubes (SWCNTs) have drawn great attention, leading to successful applications of these devices as mode-locker both into bulk solid-state and fiber ultrafast laser systems at various spectral ranges [5–8]. This is because of their advantages including fast saturation recovery time of 1ps or less, wide and easily controllable operational range and relatively simple fabrication process over the SESAM requiring sophisticated epitaxial process. The SWCNT/polymer composite directly deposited onto fiber connector ferrule are generally used to implement a compact fiber laser system. However it might potentially possess some problems such as thermal damages and mechanical damages by direct interaction with physical touching. Particularly, thermal damage accumulation due to the limited SWCNT interaction length of this scheme can be significant when the power in laser cavity considerably increases. Alternative solution using evanescent field interaction have been proposed to overcome these drawbacks by employing tapered fibers, D-shaped fibers, in-fiber micro-channels or ring core fibers [9–12]. These schemes will be beneficial for high power pulse formation by increasing the nonlinear interaction length of guided light with low concentration SWCNT/polymer composite. High power soliton laser has been reported using the SWCNT coated on D-shaped fiber [13], however it delivered multiple pulses per round trip under the conditions far from the fundamental soliton. In general, peak power and pulse duration of soliton lasers are fundamentally restricted by intra-cavity design such as dispersion and nonlinearity [14]. Other factors such as wave breaking phenomena also limit the generation of high pulse energy [15]. In recent years, new ways of high energy pulse formation at net normal dispersion of fiber laser cavity are intensively discussed and mostly

focused on the Yb-doped fiber lasers [16–18]. Several attempts have been also made in Er-doped fiber lasers based on NPE or CNT-SAs [19–21], however compact all-fiber version of Er-doped dissipative soliton laser with high power is still in challenging. Here the term of "dissipative soliton" used is originated from recent publications [22,23]. The dissipative soliton in laser cavity is one of the stable solutions found in nonlinear and dispersive medium including dissipative system described by complex Ginzburg-Landau equation [24,25], which can be more general category of recent development of high energy fiber pulse lasers at normal dispersion regime.

In the present work, we demonstrate an Er-doped dissipative soliton fiber laser based on SWCNT-SA combined with a segment of dispersion compensating fiber (DCF). A SWCNT/polymer composite film was uniformly spin-coated on side-polished fiber for several times to achieve robust and sufficient nonlinear interaction within all-fiber format. Stable evanescent field interaction with SWCNTs embedded in the polymer matrix will be more resistant to mechanical and thermal damages compared to previously reported direct coating of CNTs on D-shaped fibers [10] or SWCNT/polymer composite on fiber ferrules [5], thus favorable for high power laser operation. We investigated laser mode-locking behavior by adjustment of the cavity dispersion and observed most stable pulse formation at net group velocity dispersion (GVD) around 0.087 ps^2. The developed compact all-fiber laser delivered highly chirped 5.8 ps pulses with spectral bandwidth of 13.9 nm around 1562 nm. Measured average output power of 55.6 mW, which is much higher than few mW output reported in the previous work [21], corresponds to the pulse energy of 2.35 nJ. Preliminary experiment of pulse compression was carried out where initial pulse was compressed down to 226 fs.

2. Fabrication and characterization of the SWCNT-SA

We prepared SWCNT/polymer solution using the similar process described in Ref. 7. Commercial SWCNTs synthesized by high-pressure CO conversion (HiPCO) technique were dried and dispersed in dichlorobenzene (DCB) via ultrasonic agitation. The sample was then mixed with poly(methyl methacrylate) (PMMA) solution. We firstly measured the linear transmission of SWCNT/polymer mixture spin-coated on quartz substrates. The broadband resonant absorption distribution around near infrared wavelength originated from E_{11} transition of semiconducting HiPCO SWCNTs was observed. The side-polished fiber was then prepared for evanescent field interaction. Figure 1(a) describes its structure. A standard SMF buried into the groove of quartz block with some curvature was polished until the evanescent field appears at the central region of quartz block surface. The inset of Fig. 1(a) depicts the cross-sectional view of side-polished region. The effective interaction length of polished fiber is expected to be 2~3 mm. The fabricated side-polished fiber exhibited negligible insertion loss (less than −0.1 dB) without index oil and the loss became −12.5 dB at 1550 nm in the presence of index-matching oil on the surface. No polarization dependent behavior was observed during the measurement.

The SWCNT/polymer composite was subsequently deposited onto the side-polished fiber using a spin coater. Figure 1(b) shows the photograph image of the sample fabricated. Since the portion of electric field distributed in SWCNT/polymer depends on film thickness, the interaction with SWCNTs can be easily controlled by number of spin coating process for a given interaction length. Here we repeated spin-coating process by 5 times where almost linear relationship between number of coating and film thickness was observed. Figure 1(c) shows the surface profile of the coated film. The film thickness about 3.2 μm was measured from the substrate by alpha-step method. A little variation of layer thickness was only observed near substrate-film boundary which might occur during removing the film for the measurement of height from the substrate. Uniformly coated layer across the other area was confirmed. The transmission of the fabricated in-line SWCNT-SA varied from - 4.6 dB to −19.9 dB at 1550 nm depending on the incident polarization state as shown in Fig. 1(d). Here we intentionally fabricated the SA possessing sufficient absorption by repeated spin-coating process for facilitating mode-locking at large normal dispersion regime [20].
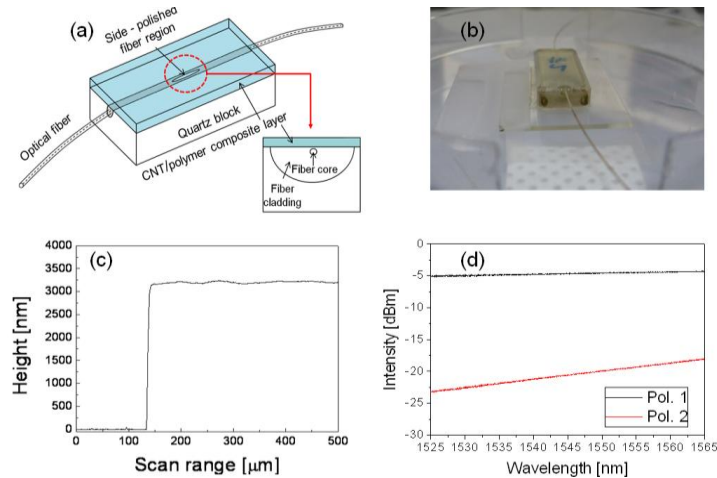
Fig. 1. (a) Schematic view of the SWCNT on side-polished fiber (b) Photograph image of the fabricated sample (c) Measured thickness of the SWCNT/polymer layer (d) Transmission characteristics of fabricated SWCNT-SA.

The SA exhibits larger loss at shorter wavelength because first resonance of E_{11} transition is centered on 1450 nm. The polarization dependent behavior is normally expected [10] because the alignment direction of SWCNTs is parallel rather than normal to the surface plane during spin coating process. The polarization sensitivity of the device can partially contribute to mode-locking operation by NPE, but we observed that mode-locking in the laser was less sensitive to polarization control compared to the case of NPE mode-locking and well sustained for broad range of pump power. Thus saturable absorption is expected to be primary for starting and stabilizing laser pulses. The investigation on the control of modulation depth and linear loss of the SA as a function of number of spin coating process are in progress.
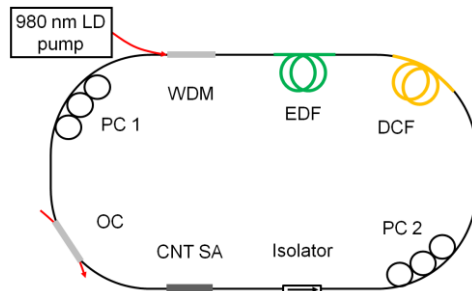

Fig. 2. Configuration of the fiber ring laser including the SWCNT-SA and the DCF.

3. Fiber laser experiment and discussion

The fiber ring laser was built by incorporating the fabricated SWCNT-SA as depicted in Fig. 2. A 980-nm laser diode (LD) was used for pumping the highly Er-doped fiber (EDF) with a length of 2m via a wavelength division multiplexing (WDM) coupler. Two polarization controllers (PCs) were employed to adjust the state of polarization for the SA and the laser cavity. The propagating light in the cavity was extracted from the 3 dB output coupler (OC). The fabricated SWCNT-SA was placed in the laser cavity and an isolator follows it for unidirectional operation of the ring laser. A 1.8-m-long dispersion compensating fiber (DCF) was employed to form a normal dispersion cavity. All fibers used in the laser cavity were composed of standard SMF (SMF28e®) except for a segment of EDF, DCF and HI1060 (0.25 m) used for WDM coupler. The dispersion of β_2 of each fiber was estimated to be 163.2,

−22.3 and −11.2 ps^2/km for DCF, EDF and HI1060, respectively. Net GVD of the cavity is adjusted by additional standard SMF.

The experiment was carried out near net zero dispersion of the laser cavity. Unstable pulse formation was observed from total dispersion of the cavity of 0.018 ps^2 at pump power of 365 mW. Figure 3(a) and 3(b) represents the spectrum and the pulse property of laser output under given conditions. The inset of Fig. 3(b) indicates single pulse formation per round trip of laser cavity from the measurement using a high speed detector. The intensity autocorrelation measurement in Fig. 3(b) indicates that the pulse of laser output includes significant portion of very broad noisy background. The steep edges of the autocorrelation trace are due to the limited measurement range of our autocorrelator. The unstable operation of main pulse such as timing jitter was also observed.
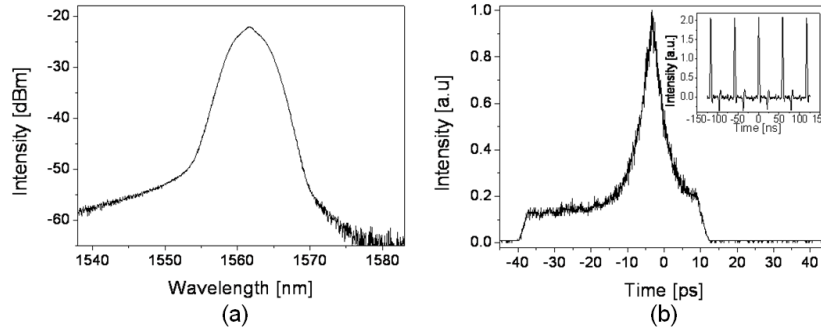

Fig. 3. (a) Output spectrum and (b) intensity autocorrelation trace (inset: pulse train measured by high speed detector) of the fiber ring laser at the net cavity dispersion of 0.018 ps^2.

We then increase the net cavity dispersion by reducing the length of the SMF. Stable pulse formation was observed from the net cavity dispersion of 0.075 ps^2. Figure 4(a) shows the spectrum at the dispersion of 0.087 ps^2 where the maximum spectral bandwidth of 13.9 nm was achieved at central wavelength of 1561.8 nm. Stable and self-starting mode-locking starting from the pump power of 250 mW was well sustained during the laser operation of many hours. The maximum output power achieved was 55.6 mW at the maximum pump power of 430 mW, which corresponds to the pulse energy of 2.35 nJ at the measured repetition rate of 23.6 MHz.
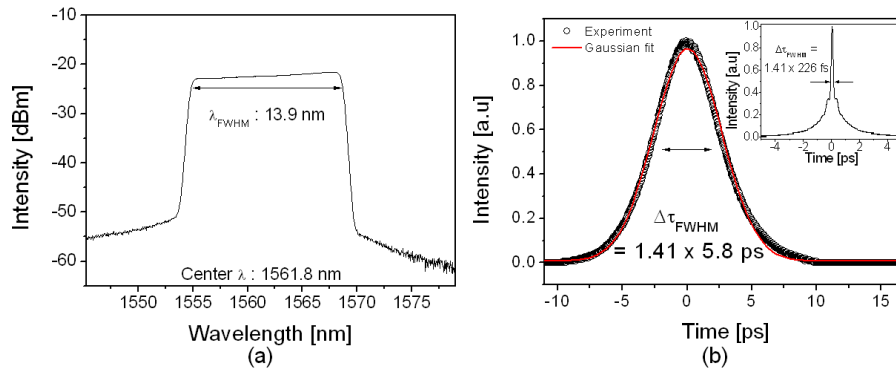

Fig. 4. (a) Optical spectrum of the mode-locked laser at net cavity dispersion of 0.087 ps^2 and (b) Measured pulsed duration fitted with Gaussian pulse. The inset shows the pulse compressed by additional SMF at extra-cavity.

In our experience, the fiber laser using the SWCNT-SA on fiber ferrule typically underwent degradation at the output power level more than few mW when concentration of SWCNTs is high for realizing large modulation depth of SA. Current SWCNT-SA coated on side-polished fiber did not exhibit the signature of deterioration regardless of CNT

concentration during our repeated experiments for few months. In Fig. 4(b) the measured pulse duration is well fitted with Gaussian pulse shape. The full width half maximum (FWHM) of the pulse was measured to be 5.8 ps, which is about 23 times of the value of a transform-limited pulse. The laser output was then compressed by employing conventional SMF at extra-cavity. The inset of Fig. 4(b) shows the measured pulse compressed down to 226 fs at FWHM. Although large majority of energy still resides in wings (estimated root-mean square of pulse width is about 1.6 ps), it can be improved by using a large-mode area fiber at extra-cavity to suppress the nonlinear pulse propagation. The laser output characteristics experimentally achieved are well compared with the previous theoretical expectation [26,27] particularly for steep edges in spectrum with highly chirp pulse at large normal dispersion regime though the behavior near zero dispersion are not clearly understood at present.

Figure 5 represents the characteristics of the pulse train measured by radio-frequency (RF) spectrum analyzer. The fundamental beat note of 23.6 MHz corresponding to the laser cavity length about 8.6 m was measured with an extinction ratio of −68.3 dBc from noise level. The inset of Fig. 5 shows wide span measurement of the spectrum including harmonics of fundamental repetition rate, which indicates stable single-pulse mode-locking.
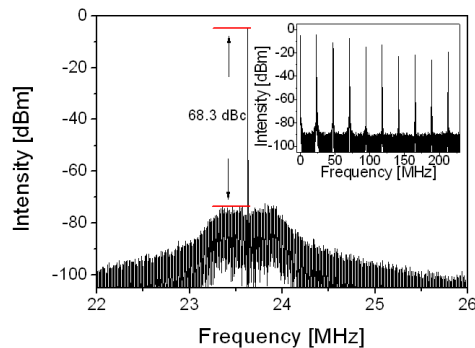

Fig. 5. RF spectrum of fundamental beat note and high harmonics (inset).

4. Summary

We demonstrated all-fiber Er-doped pulse laser at net normal dispersion regime using SWCNT-SA on side-polished fiber combined with a DCF. The evanescent field interaction with SWCNTs embedded in polymer provided robust and long nonlinear interaction, which can increase damage threshold of SA device for high power operation. Stable pulses with pulse energy of 2.35 nJ were formed at laser cavity dispersion of 0.087 ps^2 where average output power was measured to be 55.6 mW. The developed all-fiber fiber pulse laser possessed steep spectral edges with 13.9 nm bandwidth around 1561.8 nm, and delivered chirped pulse of 5.8 ps duration compressed down to 226 fs. Further investigation on modulation depth and linear loss control of our SA will enable compact and stable all-fiber lasers delivering higher power pulses more than hundred mW at various spectral ranges.